

# CrystEngComm

Accepted Manuscript



This is an *Accepted Manuscript*, which has been through the Royal Society of Chemistry peer review process and has been accepted for publication.

*Accepted Manuscripts* are published online shortly after acceptance, before technical editing, formatting and proof reading. Using this free service, authors can make their results available to the community, in citable form, before we publish the edited article. We will replace this *Accepted Manuscript* with the edited and formatted *Advance Article* as soon as it is available.

You can find more information about *Accepted Manuscripts* in the [Information for Authors](#).

Please note that technical editing may introduce minor changes to the text and/or graphics, which may alter content. The journal's standard [Terms & Conditions](#) and the [Ethical guidelines](#) still apply. In no event shall the Royal Society of Chemistry be held responsible for any errors or omissions in this *Accepted Manuscript* or any consequences arising from the use of any information it contains.



Tris (8-hydroxyquinoline) aluminium ( $\text{Alq}_3$ ) is one of the commonly used metal-organic materials for the OLED technology. The interest in  $\text{Alq}_3$  does not decrease at the background of synthesized new and sometimes more effective organic semiconductors. In commercial products the purity for sublimated  $\text{Alq}_3$  is usually indicated being not higher than 99.995 wt.% trace metals basis<sup>11</sup>, but its phase purity including polymorphic phases is not mentioned at all.

The  $\text{Alq}_3$  molecule is known to exist in two isomers – facial (*fac*) and meridional (*mer*) and on their basis several polymorphs are formed in a crystalline phase depending on the temperature. The following general scheme of polymorphic transitions in  $\text{Mq}_3$  (M= Al, Ga, In) vs relative temperature was proposed for the preparations with the purity 99.995 wt.%<sup>15</sup> (Fig.1). We defined T1 more accurately in the present research using extra pure  $\text{Alq}_3$ . It was found to be  $(0,66\pm 0,1)\times T_m$  ( $\text{Mq}_3$ ). The number and the temperatures of polymorphic transitions varied considerably, according to different authors<sup>14,15,16</sup>.

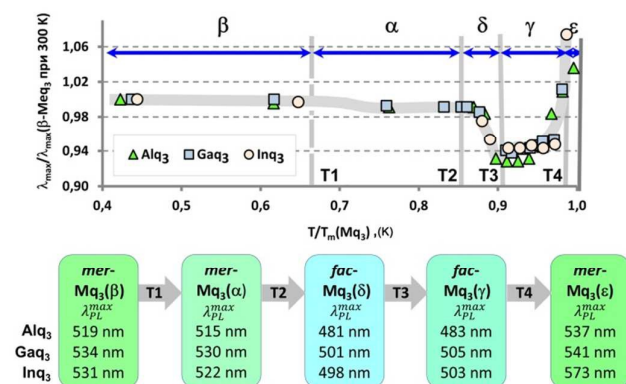


Fig. 1 Relative PL maximum vs relative temperature for different polymorphs (top) and scheme of polymorph transitions (bottom) of  $\text{Mq}_3$  (M=Al, Ga, In)<sup>15</sup>.

If the purity of the material is not taken into account, this contradiction can be explained by the synthesis conditions and the composition of the compound based on deviations from stoichiometry, which is a common case for inorganic crystalline phases<sup>18</sup>. Establishing the relationships between the synthesis conditions (temperature, partial vapour pressure of ligand-forming compounds) and structurally-sensitive properties of different polymorphic modifications of electroluminescent metal-organic compounds will allow formulating the requirements for developing the technology of organic semiconductor materials of a new generation of electronics and photonics.

From the point of view of solid-state chemistry,  $\text{Alq}_3$  is considered to be a molecular crystal. Molecular crystals are believed to have a fixed stoichiometric composition<sup>19</sup>. However, as the thermodynamic laws characteristic of inorganic crystals refer to  $\text{Alq}_3$ , the phenomenon of nonstoichiometry may be assumed to be detected in the given crystalline material, as well. Until now, the phenomenon of crystal structure at the level of point defects inherent in inorganic substances has not been discussed with respect to the crystalline phases based on metal-organic compounds. In

the present research we have attempted to answer the question if the phenomenon of nonstoichiometry occurs in the studying metal-organic crystals of  $\text{Alq}_3$  as an example.

## Experimental

### Synthesis and purification of $\text{Alq}_3$ complex.

The synthesis of tris (8-hydroxyquinoline) aluminium was conducted in isopropanol (pH = 10) at 50°C and continuous mixing for 1h. 1.63 g of  $\text{Al}(\text{NO}_3)_3$  water solution was added drop wise to a stirred warm solution of 1.90 g of the 8-hydroxyquinoline (8-Hq) in 50 ml isopropanol, which was followed by the addition of 3 ml  $\text{NH}_4\text{OH}$  solution until pH = 9. The mixture was maintained for 1 h at constant stirring and heating, and then it was cooled and filtered. The separated precipitate was washed with two portions of n-hexane. The obtained material was represented as a light yellow powder. It was purified by vacuum sublimation in diffusion pump system (DP) ( $P < 10^{-6}$  Torr) and magnetic discharged (Ti) system (MD) ( $P < 10^{-5}$  Torr). Diffusion pump system provides  $\text{Alq}_3$  purity, which corresponds to that of the product offered by Sigma-Aldrich<sup>11</sup> – 99.995 wt.% trace metal basis.  $\text{Alq}_3$  powder samples purified by vacuum sublimation in the DP system had purity higher than  $\text{Alq}_3$  for the MD system. The powders were as pure as 99.9950% and 99.9987% respectively by means of ICP-MS analysis (NexION300D, PerkinElmer Inc.) (see Supplementary, Table S1).

### Burdon manometer technique.

8-hydroxyquinoline (8-Hq) is a well-known compound which has been used as a complex agent for detecting trace amounts of many metals. However, at present the data on 8-Hq partial pressure above the melting point have not been found yet. So, the Burdon technique was used to determine the  $P_{8\text{-Hq}} = f(T)$  dependence. The research was conducted at 386-482 K temperature range using the 8-Hq powder of the 99.998% wt.% purity measured by ICP-MS (NexION300D, PerkinElmer Inc.). The experiment was performed in an evacuated glass ampoule (0.1 Torr). Heating was provided by immersing the reaction ampoule in a low-melting Wood alloy ( $T_m = 341.5$  K). The pressure was measured by a mercury U-manometer with accuracy 0.05 Torr.

### Crystals growth of $\text{Alq}_3$ .

In the case of a binary compound during a nonstoichiometry investigation a crystal is synthesized under bivariant ( $S_{ABV}$ ) or monovariant ( $S_{ABLV}$ ) conditions<sup>18</sup>. However,  $\text{Alq}_3$  is a multicomponent chemical compound consisting of H, C, O, N, and Al. In practice, it is impossible to fix the four intensive thermodynamic parameters to control the  $S_{\text{Alq}_3V}$  bivariant equilibrium and synthesize a single-phase material. The problem could be solved by consideration of  $\text{Alq}_3$  as a quasi-binary compound consisting of Al as a coordinating atom and 8-Hq as a ligand-forming substance. In this case,  $\text{Alq}_3$  can be annealed at a fixed temperature and partial pressure of 8-Hq ( $P_{8\text{-Hq}}$ ) to produce a single-phase sample.

The duration of the Alq<sub>3</sub> annealing process to achieve a thermodynamically equilibrium state could be very long because of the comparatively low operating temperature and the large size of the ligand. Accordingly, the conditions were selected for the crystal growth under controlled P<sub>8-Hq</sub> using evacuated quartz glass ampoule (10<sup>-5</sup> Torr) placed in a two-zone gradient furnace (Fig. 2). To reduce the rate of Alq<sub>3</sub> sublimation appropriate for high quality crystal growth we filled an ampoule with extra pure Ar, which pressure depended on the controlled P<sub>8-Hq</sub> within 1-10 Torr range. Varying P<sub>Ar</sub> we achieved the situation at which the Alq<sub>3</sub> crystals were grown (condensed on the ampoule walls) at a fixed temperature zone 483±5 K. At these temperatures the Alq<sub>3</sub> did not dissociate in vapour and 8-Hq does not decompose in vapour<sup>17</sup>. The synthesis conditions of the grown crystals are presented in Table 1.

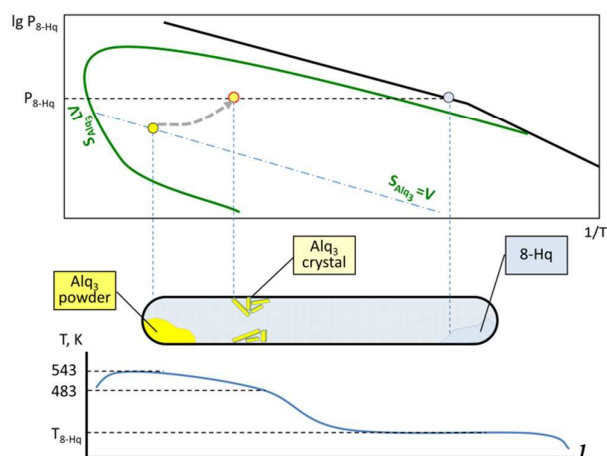


Fig. 2 Schematic diagram of the growth and annealing of Alq<sub>3</sub> crystal in S<sub>Alq<sub>3</sub>V</sub> bivariate equilibrium at 8-Hq fixed vapor pressure.

Table 1 The synthesis conditions of the grown crystals

Sample number	T <sub>cryst,Alq<sub>3</sub></sub> , K ±5	τ, h	T <sub>8-Hq</sub> , K	P <sub>8-Hq</sub> , Torr
1	483±5	55	—*	—
2	480±5	57	320	0.146
3	483±5	66	341	0.542
4	479±6	62	369	2.476
5	478±6	47	374	3.170
6	481±4	65	387	5.852
7	480±6	64	388	6.124
8	481±5	63	402	11.30

\* congruent sublimation conditions

### OLED structures manufacturing.

The multilayers OLED devices were fabricated by layer-by-layer vacuum thermal sputtering on a glass substrate (20x30x3 mm) with ITO conducting layer. The deposition rates of each layer were no more than 0.02 nm·s<sup>-1</sup>. The device configuration was ITO/MoO<sub>3</sub> (1 nm)/TPD (40 nm)/Alq<sub>3</sub> (40 nm)/LiF (1.2 nm)/Al (100 nm). MoO<sub>3</sub> is a hole blocking material which we specially prepared as an extra pure material (99.9995 wt.% with W concentration <8×10<sup>-5</sup> wt.%) with controlled nonstoichiometry<sup>18</sup>. TPD (99%, Sigma Aldrich) is one of the

most efficient hole-transport materials for providing the necessary hole mobility<sup>4</sup>.

### X-ray crystallography of Alq<sub>3</sub>.

The powder patterns were measured on Bruker D8 Advance diffractometer with LynxEye detector and Ni filter, λ(CuKα) = 1.5418 Å, θ/2θ scan from 18° to 120°, step size 0.01°, in Bragg-Brentano geometry, with the sample deposited on Si plate. About 20% of silicon powder was added to every sample as internal standard. The powder patterns were refined in TOPAS 4.2 software<sup>27</sup>. All peaks correspond to the literature structure of α-(mer)-tris(8-hydroxyquinoline)-aluminum(III)<sup>12,13</sup>. Lattice parameters were refined with Pawley technique, lattice parameter of Silicon was fixed to 5.431179 Å.

### Luminescence measurements.

All of the luminescence measurements were carried out at room temperature. A Fluorolog FL3-22 spectrofluorimeter (Horiba Jobin Yvon) with double-grating excitation and emission monochromators was used for luminescence measurements over a wavelength range of 400 to 700 nm with a 0.1 nm step. Deconvolution of the PL spectra was carried out with OriginPro 8 SR4 software using the Fit Multiple Peak procedure. The luminescence decay kinetics were studied by the excitation of a pulsed diode laser (λ = 377 nm, Δt = 1.5 ns) and a Xenon 450W Ushio UXL-450S/O lamp (355 nm). Processing of the luminescence decay curves was carried out with OriginPro 8 SR4 software using the Fit Exponential procedure. All of the decay curves were described by two exponentials (criterion Adj. R-Square N≥0.999). The final data were averaged over 5 measurements.

### OLED structures Luminescence Measurements.

OLED structures luminescence measurements such as brightness and chromaticity coordinates of were measured by a LumiCAM 1300 photo-colorimeter (Instrument Systems Optische Messtechnik, GmbH). In the case of EL OLED structures were activated by a direct current which was determined by an applied voltage and the structure resistivity. EL spectra of the devices were measured by QE65000 spectrometer (Ocean Optics, Inc.).

## Results and discussion,

### Partial pressure of 8-hydroxyquinoline.

Comparison of the achieved data for vaporization of 8-Hq in the 386-481 K temperature range (Fig. 3, Table 2) with the results of 8-Hq sublimation in the 298.18-303.45 K temperature range<sup>20</sup> made it possible to determine the melting temperature of 8-Hq (350.7±0.7 K for 8-Hq preparation with 99.999 wt.% purity), which is consistent with the reference data (345.74±0.15 K for 8-Hq preparation with 99.5 wt.% purity<sup>21</sup>; 348±2 K for 8-Hq preparation with 99.8 wt.% purity<sup>22</sup>). The experimental data results to the following equation

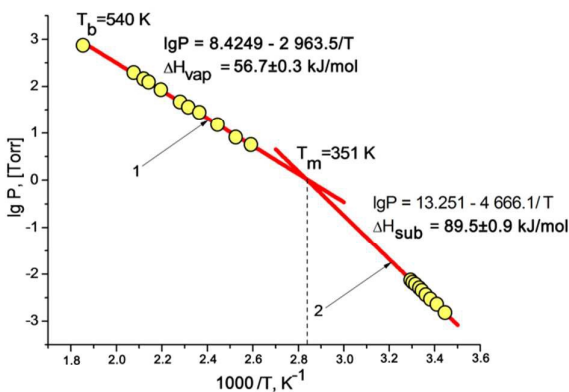


**Fig. 3** The vapor pressure of 8-hydroxyquinoline vs reciprocal temperature: 1 – vaporization data, measured by Burdon manometer technique; 2 – sublimation data obtained by Knudsen effusion technique<sup>20</sup>.

$$\lg P_{8\text{-Hq}} = -(2963.5 \pm 43.1)/T + (8.42494 \pm 0.09797) \text{ [Torr]}$$

**Table 2** Pressure of 8-hydroxyquinoline measured by Burdon manometer technique at different temperatures

$T_3$ , K	$P_{8\text{-Hq}}$ , Torr	$T_3$ , K	$P_{8\text{-Hq}}$ , Torr
386.45	5.5	455.45	88.0
396.15	8.0	467.15	125.8
408.95	15.2	472.45	150.3
422.95	27.5	481.95	196.0
431.85	36.3	539.75	752 <sup>28</sup>
438.45	47.2		

According to  $\lg P = f(1/T)$  dependence we determined both the enthalpy of vaporization ( $56.7 \pm 0.3 \text{ kJ} \times \text{mol}^{-1}$ ), and the enthalpy of sublimation ( $89.5 \pm 0.9 \text{ kJ} \times \text{mol}^{-1}$ )<sup>20</sup> as well as the melting heat

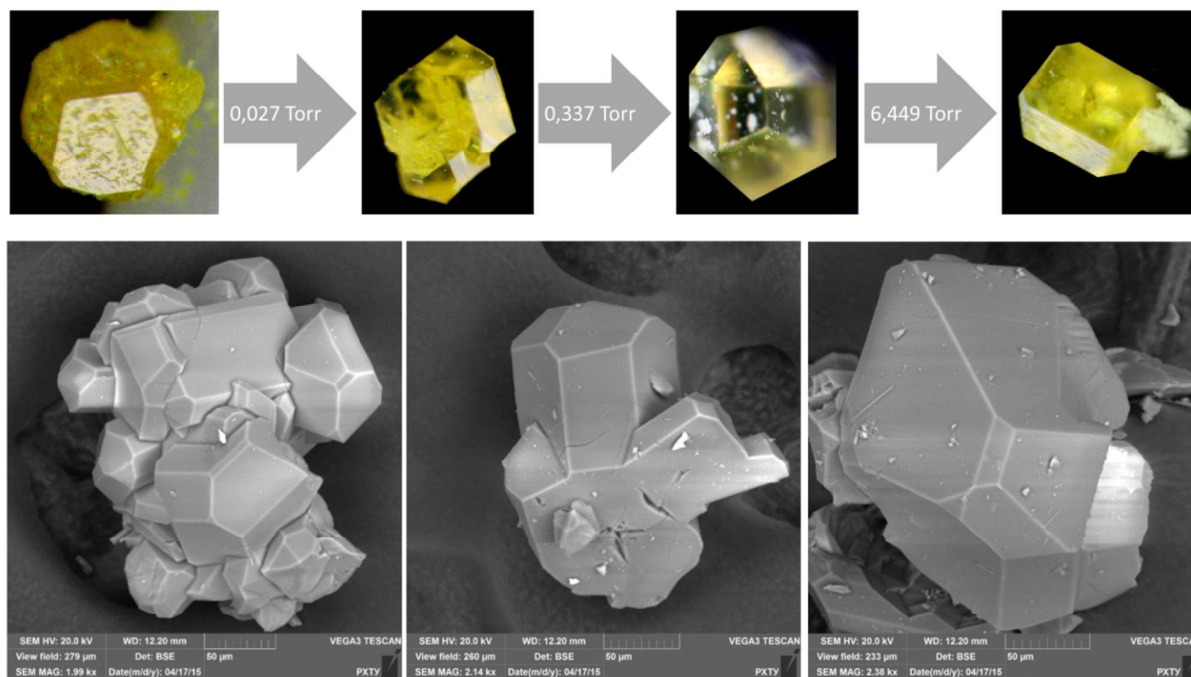
of  $32.6 \pm 1.7 \text{ kJ} \times \text{mol}^{-1}$ .

### Structural properties of $\text{Alq}_3$ crystals.

The  $\text{Alq}_3$  crystals grown under different 8-Hq partial pressures were studied by XRD technique and the cell parameters were estimated (Table 3). According to XRD results, all crystals were attributed to the  $\alpha\text{-Alq}_3$  polymorph which correlated with the  $\beta \rightarrow \alpha$  phase transition temperature (see Fig.1), but their parameters were not equal. The  $\alpha\text{-Alq}_3$  polymorph belongs to the triclinic space group  $P\bar{1}$  and the crystals had various habitus (Fig. 4).

Simultaneously with crystal growth we made experiments in which powdered  $\text{Alq}_3$  was annealed at the same condition. PXRD of these preparations did not show any presence of other polymorphs except  $\alpha\text{-mer}\text{-Alq}_3$  and the cell parameters were within the accuracy of those of the grown crystals.

Besides, the crystal lattice parameters were different for all crystals, the cell volumes as an integrated parameter of the crystal lattice were compared (Fig. 5) and its systematic decrease at the  $P_{8\text{-Hq}}$  increase was found. The given decrease was much more than the determination accuracy for the cell volume. It was assumed to be a result of generation of point defects in the crystal lattice. The term 'point' should be understood as a local change in crystal lattice periodicity at Al atom or ligand levels<sup>18</sup>. By analogy with inorganic semiconductors the lattice volume reduction can be explained by the generation of vacancies in any sublattice. The probability of vacancy generation in Al-sublattice was higher compared to the ligand sublattice because the volume decrease at 8-Hq partial pressure increase took place.

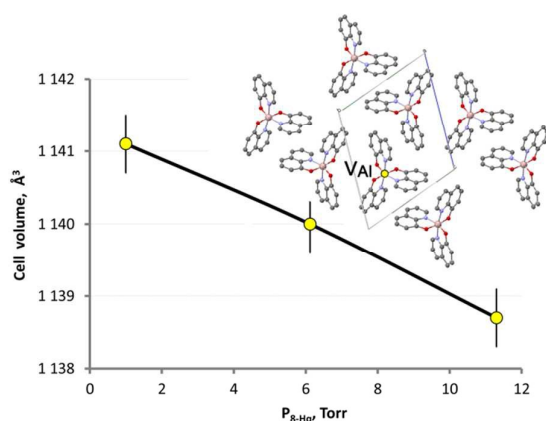


**Fig. 4** Photo (a top row) and SEM images of  $\text{Alq}_3$  crystals (a bottom row) grown at  $T = 483 \text{ K}$  under  $S_{\text{Alq}_3} = V$  congruent sublimation (left) and the partial pressure of 8-hydroxyquinoline 0.542 Torr (in the middle) and 6.124 Torr (on the right).

**Table 3** Structure parameters of Alq<sub>3</sub> crystals grown at different partial pressures of 8-hydroxyquinoline (Sample numbers are listed in Table 1)

Parameter	Crystal sample number		
	1	7	8
Space group	$P\bar{1}$	$P\bar{1}$	$P\bar{1}$
a (Å)	6.4474(13)	6.445(3)	6.4466(12)
b (Å)	12.9050(13)	12.902(2)	12.8958(12)
c (Å)	14.7715(14)	14.768(2)	14.7661(14)
alpha (°)	110.159(7)	110.179(13)	110.265(7)
beta (°)	88.650(14)	88.53(4)	88.618(15)
gamma (°)	98.32(2)	98.34(4)	98.42(2)
Cell Volume (Å <sup>3</sup> )	1141.1(3)	1140.0(6)	1138.7(3)

The analysis of SEM images of the crystals has shown that the phase contrast (i.e. the flux of backscattering electrons) of the grown crystals at a higher pressure of 8-Hq is greater (brightness is lower) and it indicates a lower average Z number on the crystal surface or lower surface electrical conductivity<sup>26</sup> (Fig. 4 bottom row). This is consistent with the hypothesis about the presence of vacancy defects in the aluminum sublattice, which generate free charge carriers in a crystal. Thus, the crystals with a higher concentration of vacancies will have a higher conductivity and a lower brightness of SEM image.

**Fig. 5** Cell volumes of Alq<sub>3</sub> crystals grown under different P<sub>8-Hq</sub> at 483 ± 5 K and the proposed packing structure of α-Alq<sub>3</sub> with Al atoms deficit (i. e. aluminum vacancies V<sub>Al</sub>).

The aluminum deficit could cause some changes both in electrical and luminescent properties of Alq<sub>3</sub> crystals.

#### Luminescent properties of Alq<sub>3</sub> crystals.

The photoluminescent (PL) spectrum of α-Alq<sub>3</sub> has been described in detail<sup>23,24</sup>. A PL spectrum is very sensitive to negligible changes in the concentration of impurities or other structure defects including point defects<sup>18</sup>. The small changes in the PL peak parameters vs P<sub>8-Hq</sub> (Fig.6, Table 4) indicate that

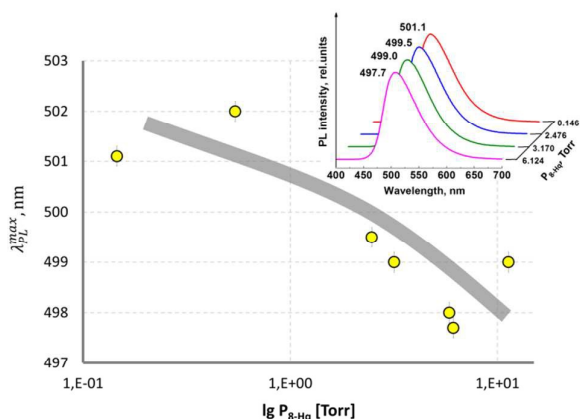
the concentration level of the supposed Al-vacancies is rather low and it did not allow measuring the difference in the Al gross concentration of Alq<sub>3</sub> vapor grown crystals. This is an ordinary situation which is a real challenge for the modern analytical chemistry when the deviation from stoichiometry is less than 10<sup>-2</sup> mol.%<sup>25</sup>.

**Table 4** Photoluminescent properties of Alq<sub>3</sub> single crystals grown under different P<sub>8-Hq</sub>

N	P <sub>8-Hq</sub> , Torr	Center, nm	Centroid, nm	Area	FWHM, nm
1	—*	498.7	517.26	87.536	81.62
2	0.146	501.1	520.35	81.614	74.62
3	0.542	502.0	522.38	83.327	76.13
4	2.476	499.5	516.33	88.096	82.07
5	3.170	499.0	515.46	86.250	80.26
6	5.852	498.0	516.35	85.792	79.26
7	6.124	497.7	516.31	87.449	81.03
8	11.30	499.0	516.48	87.762	81.16

\* congruent sublimation conditions

All decay kinetics of PL (at 504-508 nm) for Alq<sub>3</sub> crystals grown under different P<sub>8-Hq</sub> (Fig.6, insertion) were successfully

**Fig. 6** The PL spectra of Alq<sub>3</sub> crystals grown at 483 ± 5 K under different P<sub>8-Hq</sub> (λ<sub>exc</sub> = 370 nm).

described by two exponents (see Supplementary) and the processing result presented in Table 5. This result indicates the existence of two types of centers responsible for luminescence, which could be attributed with some states in the Alq<sub>3</sub> molecule existing in a crystal lattice field. Dependences of life-time of the every component demonstrated non-monotonic behavior at the P<sub>8-Hq</sub> increase (Fig.7).

We observed maximum of life-times between 3 and 5 Torr P<sub>8-Hq</sub>. It could be explained by changes in the symmetry of crystal field for the Alq<sub>3</sub> crystals with a different content of Al

vacancies (see Fig 5 insertion). The ratio of long-lived and short-lived centers ( $A2/A1$ ) (Table 5) demonstrated nearly monotonic decrease with the  $P_{8-Hq}$  similar to the  $\lambda_{pl}^{max}$  behavior (Fig.6).

The observed hypochromic shift of  $\lambda_{pl}^{max}$  could be explained by a loosened molecular orbitals interaction at the Al vacancies presence. This result correlates with the bathochromic shift in 100 nm of  $\lambda_{pl}^{max}$  observed under 7.5 GPa high static pressure<sup>29</sup> which the authors explained by a decreasing of intermolecular distances and strengthening of molecular orbitals interaction.

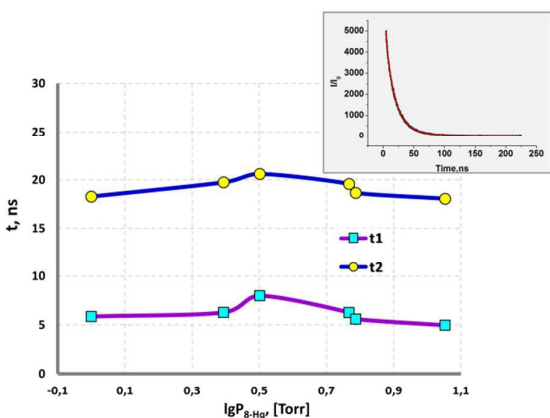


Fig. 7 Life times ( $t_1$  and  $t_2$ ) of PL decay kinetics (insert) for  $Alq_3$  crystals prepared under different  $P_{8-Hq}$ , and processed by the equation:  $Y = A1 \times \exp(-x/t_1) + A2 \times \exp(-x/t_2) + Y_0$

#### The electroluminescent properties of OLED structures.

The electroluminescence (EL) structures brightness is more dependent on the purity of organic metal complexes than that of the organic phosphors PL. So, the experiments were

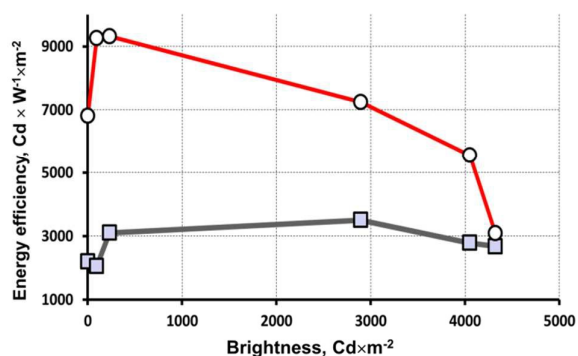


Fig. 8 Energy efficiency of OLED structures with topology ITO/MoO<sub>3</sub>(1nm)/NPD(40nm)/Alq<sub>3</sub>(60nm)/LiF(1,2nm)/Al(100nm) when used as an emission agent  $Alq_3$  powders with a purity of 99.9950 wt.% (○) and 99.9987 wt.% (□).

conducted to study the influence of metal-organic complexes purity including Al-atoms' deficit on the EL brightness.  $Alq_3$  powder samples purified by vacuum sublimation in diffusion pump system (DP) ( $p < 10^{-6}$  Torr) had a purity higher than  $Alq_3$  from magnetic discharged (Ti) system (MD) ( $p < 10^{-5}$  Torr). The powders were as pure as 99.9950% and 99.9987%, respectively, according to ICP-MS analysis (NexION300D, PerkinElmer Inc.). The OLED structure produced on the basis of these  $Alq_3$  preparations showed threefold difference in energy efficiency (Fig. 8).

The analysis of the characteristics of OLED structures prepared using the  $Alq_3$  powder preparations, synthesized under the different  $P_{8-Hq}$  showed significant differences in the distribution uniformity and the brightness value (Fig. 9). In general, the characteristics are improved when using  $Alq_3$ , synthesized under a higher  $P_{8-Hq}$ .

#### Conclusions

By means of vapour deposition at controlled partial vapour pressures of 8-hydroxyquinoline ( $P_{8-Hq}$ )  $\alpha-Alq_3$  crystals were grown and their luminescent and structural properties were studied. An increase in the  $P_{8-Hq}$  was found to lead to a shift of the photoluminescence peak maximum, a change in PL decay kinetics, and significant changes in the unit cell volume of the  $\alpha-Alq_3$  crystals. The achieved results can be explained by the formation of a thermodynamically equilibrium crystal structure, which depending on the  $P_{8-Hq}$  leads to a change in a number of Al atoms at the constant amount of ligands in the crystal structure. This phenomenon for inorganic crystal is known as nonstoichiometry and for metal organic crystal has not been described yet.

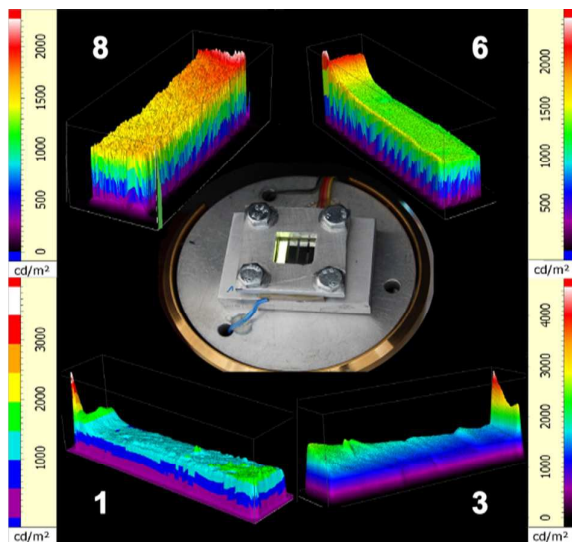
Table 5 Results of decay kinetics processing using the following equation  $Y = A1 \times \exp(-x/t_1) + A2 \times \exp(-x/t_2) + Y_0$

P, Torr	lg P, Torr	Y0	A1	t1	A2	t2	A2/A1
1.00	0.00	35.17±0.62	1889.23±38.63	5.86±0.24	5308.13±55.61	18.28±0.09	2.810
2.48	0.39	27.48±0.66	1971.68±36.71	6.27±0.22	5143.74±52.82	19.74±0.10	2.609

3.17	0.50	35.10±0.76	1677.38±72.20	7.97±0.36	4989.87±89.42	20.60±0.15	2.975
5.85	0.77	29.40±0.65	1869.36±36.89	6.27±0.22	5109.44±52.26	19.58±0.10	2.733
6.12	0.79	39.81±0.65	1917.03±35.40	5.60±0.21	5237.27±47.99	18.66±0.09	2.732
11.30	1.05	39.55±0.63	2574.90±44.37	4.95±0.15	5072.86±41.73	18.05±0.08	1.970

## Acknowledgements

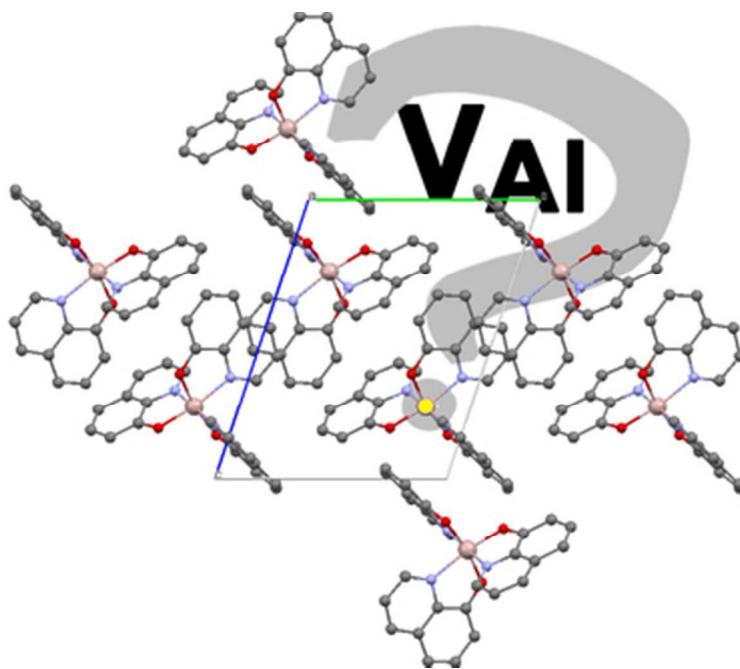
The research was supported by the Russian Foundation for Basic Research; Contract no. 16-32-60035 and the Ministry of Science and Education of Russia (grant 14.577.21.0146).



**Fig. 9** Three-dimensional maps of electroluminescence intensity of OLED devices [ITO/MoO<sub>3</sub> (1 nm)/NPB (35 nm)/ Alq<sub>3</sub> (40 nm)/ LiF (1.2 nm)/ Al (100 nm)] with Alq<sub>3</sub> emitting layer at 4.5 V applied voltage.

## References

- K. Müllen, U. Scherf, *Organic Light-Emitting Devices: Synthesis, Properties, and Applications*, Wiley-VCH, 2006.
- R. Mertens, *The OLED Handbook. A Guide to OLED Technology, Industry and Market*. 2014.
- Z. Li, in H. Meng (Eds.), *Organic Light-Emitting Materials and Devices*, CRC Press, Taylor and Francis Group, 2007.
- S. Franky, in: S. Franky (Ed.), *Organic Electronics: Materials, Processing, Devices and Applications*, Taylor and Francis Group, Boca Raton, 2010.
- S. Yanagisawa, K. Lee and Y. Morikawa, *J. Chem. Phys.*, 2008, **128**, 244704.
- G. Baldacchini, T. Baldacchini, A. Pace and R. B. Podec, *Electrochemical and Solid-State Letters*, 2005, **8** (10), J24-J26.
- G. Baldacchini, T. Baldacchini, P. Chiacchiaretta, A. Pace and R.B. Podec, *J. Electrochem. Soc.*, 2007, **154** (7), J217-J225.
- N.Audet and M.Cossette, *JEM*, 2011, **34** (6), 683-686.
- A. West, *Solid State Chemistry*, 2nd Edition, Student Edition, Wiley, 2014 (ISBN: 978-1-119-94294-8).
- I. Avetissov. E. Mozhevitina. A. Khomyakov, and R. Avetisov, *Cryst. Res. Technol.*, 2015, **50** (1), 115.
- <http://www.sigmaaldrich.com/catalog/search?term=Tris-%288-hydroxyquinoline%29aluminum&interface=Product%20Name&N=0+&mode=mode%20matchpartialmax&lang=en&regio>
- n=RU&focus=productN=0%20220003048%20219853286%20219853229 (date of the application 19.12.2015)
- T. Blanton, C. Barnes, J. Putrelo, A. Yeboah and S. Switalski, *Powder Diffraction*, 2004, **19** (01), 36-39.
- M. Cölle and W. Brütting, *Phys. Stat. Sol. (a)*, 2004, **201** (6) 1095.
- M. Brinkmann, G. Gadret, M. Muccini, C. Taliani, N. Masciocchi and A. Sironi, *J. Am. Chem. Soc.*, 2000, **122**, 5147.
- R.I. Avetisov, O.B.Penrova, A.A. Akkuzina, A.V. Khomyakov, R.R. Saifutyarov A.G. Cherednichenko, T.B.Sagalova, N.A. Makarov, and I.Kh. Avetisov, *Russian Microelectronics*, 2014, **43**(8), 526-530.
- M. Cölle, J. Gmeiner, W. Milius, H. Hillebrecht, and W. Brütting, *Adv. Func. Mater.*, 2003, **13**(2), 108-112
- D.M. Peiris, w. Lam, S. Michael, and R. Ramanathan, *J. Mass. Spectr.*, 2004, **39**, 600-606
- F. A. Kroger, *The Chemistry of Imperfect Crystals*, Amsterdam, North-Holland Pub. Co.; New York, Interscience Publishers, 1964.
- E. A. Siliush, *Organic Molecular Crystals: Their Electronic States*, Springer Science & Business Media, 2012.
- M.A.V.R. Da Silva, M.J.S. Monte and M.A.R. Matos, *J. Chem. Thermodyn.*, 1989, **21**, 159.
- Sh.-X. Wang, Zh.-Ch. Tan, Y.-Sh. Li, B. Tong, Y. Li, Q. Shi and J.-N. Zhang, *Chinese J. Chem.*, 2008, **26**, 2016.
- <http://www.odysseychem.net/products/148-24-3.htm> (date of the application 19.12.2015).
- M. Muccinia, M. Brinkmann, G. Gadret, C. Taliani, N. Masciocchi and A. Sironi, *Synthetic Metals*, 2001, **122**, 31-35.
- A. Degli Esposti, M. Brinkmann and G. Ruani, *J. Chem. Phys.*, 2002, **116**, 798.
- I. Avetissov. E. Mozhevitina. A. Khomyakov and Tran Khanh, *Cryst. Res. Technol.*, 2015, **50** (1), 93.
- R. F. Egerton, *Physical principles of electron microscopy: an introduction to TEM, SEM, and AEM*. Springer, 2005
- Bruker TOPAS 4.2 User Manual // Karlsruhe, Germany: Bruker AXS GmbH, 2009
- Budavari, S. (ed.). *The Merck Index - An Encyclopedia of Chemicals, Drugs, and Biologicals*. Whitehouse Station, NJ: Merck and Co., Inc., 1996., p. 832
- I. Hernandez, W.P. Gillin, *J. Phys. Chem. B*. 2009, **113**(43), 14079-14086



32x27mm (300 x 300 DPI)